ILASS Americas, 22nd Annual Conference on Liquid Atomization and Spray Systems, Cincinnati, OH, May 2010

Direct Injection Multi-hole Spray and Mixing Characterization of Ethanol Gasoline Blends in Engine

Atsushi Matsumoto*, Xingbin Xie, Yi Zheng, Ming-Chia Lai
Department of Mechanical Engineering
Wayne State University
Detroit, MI 48202 USA

Wayne Moore
Advanced Powertrain
Delphi Corporation
3000 University Dr.
Auburn Hills, MI 48326 USA

Abstract

Combination of GDi and ethanol has been widely studied in the automotive industry because it is able to improve fuel economy as well as emission. In a GDi engine, the spray behavior is critically related to the mixture formation, and the injection strategy must be well optimized to draw the engine's whole potential. A multi-hole injector has been found to be more suitable for a spray or wall guided GDi engine because it offers advantages of stable spray pattern and flexibility in spray plume targeting. This research employed high-speed Schlieren and Mie scattering visualization of sprays utilizing a pressurized chamber and an Optical Accessible Engine (OAE) to understand the spray behavior with various injection strategies and ambient conditions. Schlieren provided an effective technique for vapor phase visualization, and the effect of flash boiling was observed at the ambient condition of high temperature and low pressure. Once flash boiling occurred, it resulted in plume collapse and affected the spray targeting of the multi-hole injector significantly. The effect of ethanol content on the spray structure was also discussed. Earlier initiation of evaporation for gasoline fuel and resultant spray collapse was observed. Occurrence of flash boiling of the ethanol spray showed strong dependence on the fuel temperature due to its constant boiling point. OAE testing revealed that too early injection counteracted the tumble motion. The injection at the middle of the intake stroke increased the dynamic ratio and the turbulent energy at the point of ignition. Numerical simulations of the spray and mixing were carried out and the results were studied to support the experimental data.

*Corresponding author

Introduction

Gasoline Direct injection (GDi) engine has been widely studied to meet the ever-tightening emission standards and the fuel economy regulation. GDi is characterized by enhanced power and better fuel economy, improved transient response and cold-start capability.
In a side-mounted GDi engine, the injector is mounted on the cylinder wall and injects fuel directly into the combustion chamber. A GDi engine realizes less pumping loss and higher compression ratio, and better volumetric efficiency comparing to a Port Fuel Injection (PFI) engine. Detail of GDi engine was discussed in the reference [1]. It is known that a turbo charged direct injection (DI) engine is supposed to run well with ethanol fuel because of its anti-knock characteristics [2-4].

In a GDi engine, the spray behavior is critically related to the mixture formation, and the injection strategy must be well optimized to draw the engine's whole potential. Although swirl injectors had been widely studied for GDi engines [5], a multi-hole injector has been found to be more suitable for a spray or wall guided GDi engine because it offers advantages of stable spray pattern and flexibility in spray plume targeting [6, 7]. Especially, independency of spray cone angle on the ambient pressure is preferred for DI operation [8]. A multi-hole injector has been identified as a suitable solution and subject to intensive development by many fuel system and engine OEMs in recent years [9-11]. Since a GDi engine injects fuel at the compression stroke when it runs in the stratified mode, piston wetting and emission of unburned hydrocarbon and soot are the issues that need to be solved [12].

The Schlieren method is one of the most effective techniques to visualize non-homogeneous transparent flow fields, such as vapor phase of sprays. Using the Schlieren technique, it is able to visualize the change of the refraction indexes and density gradient in the object caused by material and temperature difference [13, 14].

Many studies have been done in numerical simulation of spray development and mixture formation for better understanding of the phenomena [15-18]. In spray simulation, spray breakup is a critical event and studies have been conducted to model the discrete phase of sprays. In this article, the spray behavior was predicted by a commercial code CONVERGE to support the experimental data.

In this study, high-speed spray visualization utilizing a pressurized chamber and an Optical Accessible Engine (OAE) was performed to understand the spray behavior with various injection strategies and ambient conditions. The effect of ethanol content on the spray structure was also discussed. Numerical simulations of the spray and mixing were carried out and the results were studied with the experimental data.

Experimental Setup

The high-speed visualization of spray was performed to characterize the spray structures in typical fuel injection conditions for GDi engines. The testing utilized a high-speed digital camera which speed was set to 8312 frame per second. The experiment consisted of the chamber testing and the optical accessible engine (OAE) testing.

Fig. 1 shows the experimental setup for the chamber testing. During the chamber testing, the GDi injector was fixed at the top of the test chamber which has two large windows facing each other. The chamber can be pressurized up to 3bar by the compressed air, which can be heated up to 210ºC by transmitting through a circulation heater to imitate typical engine in-cylinder conditions. At the time of injection, two valves located at the upstream and the downstream of the chamber were closed to produce quiescent ambient. Every time injection took place, the chamber was purged by the fresh air. The fuel temperature was controlled by a water jacket surrounding the injector which was capable to maintain the injector temperature between 25-80ºC. The fuel was pressurized by the compressed nitrogen at 10MPa. An injection signal was generated at the signal generator and transmitted to both the injector driver and the high-speed digital camera in order to synchronize the camera trigger to the injection.

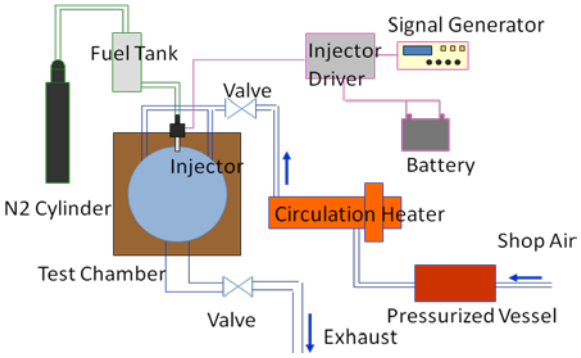

Figure 1. Experimental setup for the chamber testing.

The Schlieren setup is shown in Fig. 2. The light source was a regular projection lamp. The light coming from the source passed the pin hole, which was placed on the focal length of the first magnifying lens. The parallel light proceeded through the chamber, where the light refraction occurred, and reached the second magnifying lens. On the focal point of the lens, there was a knife edge placed to cut the refracted beam. Then the beam came into the high-speed camera, which has a resolution of 512×512 pixels (76mm×76mm).

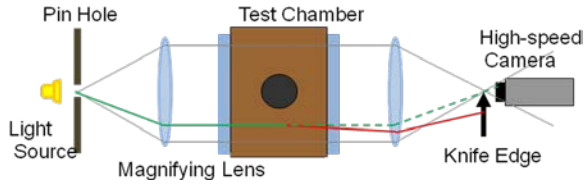

Figure 2. Schlieren visualization setup.

OAE testing can produce more realistic and dynamic in-cylinder condition. The bore and the stroke of the OAE were 86mm and 108mm respectively. The OAE was motored by a dynamometer at 1000RPM. A cylinder head taken from a production GDi engine (GM Ecotec 2.0L) was fixed on the top of the OAE. The intake and exhaust ports were open to the air. The spark plug was replaced by an in-cylinder pressure transducer. An aluminum-alloy piston reciprocated inside the quartz liner which was designed for a full-stroke optical access for the side view. The piston had two piston rings and one piston rider made by filled PTFE for better sealing without using lubricants. The OAE was equipped with crank angle degree (CAD) and top dead center (TDC) sensors. The signals were sent to a computer and Labview controlled the injection timing and duration as well as the camera trigger. The fuel was pressurized by the compressed at 10MPa.

Table 1. Fuel properties of E100, E50, and E0.

	E100	E50	E0
Density [kg/m^3]	789	764	739
Lower Heating Value (LHV) [MJ/kg]	26.8	34.7	43.1
Latent Heat of Vaporization [kJ/kg]	904		380-500
Boiling Temperature [ºC]	78.4		25-215
Research Octane Number	129		91

Three types of fuels were tested to examine the influence of ethanol content on the spray structure, which were 100% pure ethanol (E100), RON-91 gasoline (E0), and the mixture of two in 50% of volume ratio (E50). The specifications of the fuels are listed in Table 1. The differentiating properties of ethanol are its lower LHV and higher latent heat of vaporization. Since ethanol is a single component fuel, it has a constant boiling point of 78.4ºC at the standard state. Therefore the distillation curve of E100 is nearly flat and very different from gasoline's. The basic fuel was ethanol for this research, otherwise specified.

Table 2. Specifications of the tested injectors.

	A	B	C	D
Hole Diameter [mm] ×Number of Holes	0.23 ×6	0.263 ×6	0.104 ×6	0.255×1 0.259×5
Hole Length [mm]	0.31	0.3	0.23	0.28
Averaged L/D	1.36	1.14	2.21	1.1
Static Mass Flow with N-Heptane [g/s]	15.9	20.5	4.00	17.86

Four injectors in total were tested in the experiment. Injector A was a production DI injector and treated as default. The other three injectors were prototype. The specifications are summarized in Table 2. All injectors had different hole geometry, mass flow rate, and spray targeting.

Simulations of a multi-hole spray in the spray chamber and OAE were carried out with CONVERGE, a commercial 3 dimensions CFD software. The engine geometry was imported form CAD design. Although the basic grid size was 8mm, the automatic mesh refinement, such as embedded refine and Adaptive Mesh Refine (AMR), was turned on to make the finest mesh size 0.5mm at the injector tip area. The calculation time step was set to 1μs. KH-RT model [19] was chosen for the breakup model, which is a two step model of Kelvin-Helmholtz (KH) for the primary breakup and Rayleigh-Taylor (RT) for the secondary breakup. The collision and coalescence of droplets was simulated by the No Time Counter (NTC) method [20]. The rapid distortion Reynolds Averaged Navier-Stokes k-ε model [21] was used for the turbulent model.

Results and Discussions

The Schlieren visualization result with Injector A was compared with two other imaging techniques for better understanding of spray visualization. Two techniques of Mie scattering and back-lit, also known as shadow photography, have been widely adopted for spray visualization [22-24]. However, these techniques are not suitable for vapor phase visualization as Schlieren is. Fig. 3 shows the comparison of three techniques.

The images of Schlieren were able to capture the vapor cloud around the spray, which could not be detected at all in the Mie scattering images. The back-lit images showed some dark area where the vapor was supposed to be present, but it was not clear enough to insist the vapor existence. It is confirmed here that the Schlieren technique is very effective to visualize a vapor envelope of a spray as well as a dense core.

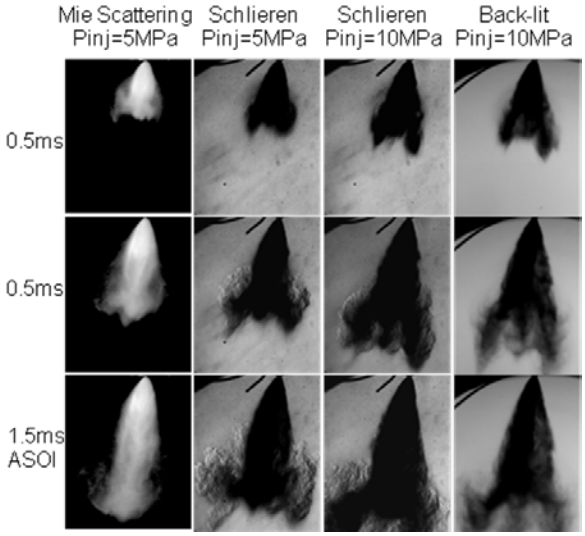

Figure 3. Comparison of visualization techniques.

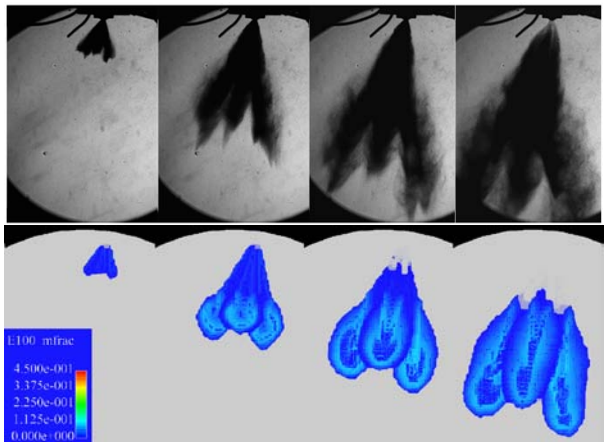

Figure 4. Comparison of experimental data and CFD at 25ºC/1bar.

Fig. 4 shows the images of the spray obtained experimentally and numerically. The simulation images show the mass fraction of ethanol vapor. The ambient condition was 25ºC with 1bar. The overall spray shape was comparable, and it is reasonable not to have the upstream portion of the spray because the amount of vapor at the upstream must be very small. The comparison of penetration with the experimental data is plotted in Fig. 5. L, M, and R in the legend indicate Left, Middle, and Right plume of the spray. The simulation fairly agreed with the experimental data, especially at the early stage of injection. However, it slightly underestimated after the break-up.

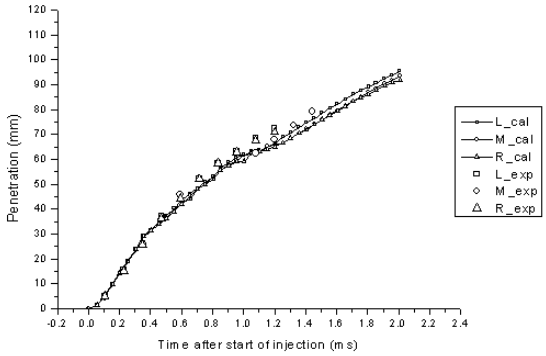

Figure 5. Penetration comparison of experimental data and CFD at 25ºC/1bar.

The effect of ambient temperature and pressure on the spray structure at 1,5ms ASOI is displayed in Fig. 6. Comparing 25ºC and 100ºC with 1bar, no significant difference in the spray shape was observed while the degree of vaporization slightly increased with the ambient temperature. However, when the ambient temperature increased over 150ºC, "flash boiling" phenomena instantly expanded the volume of the spray and could collapse the multi-hole spray into a coherent spray. Flash boiling occurs when the pressure of liquid drops instantly below the saturation pressure. It is believed that flash boiling was not observed at the higher ambient pressure because the pressure drop of the fuel was not large enough to let the fuel pressure be less than the saturation pressure.

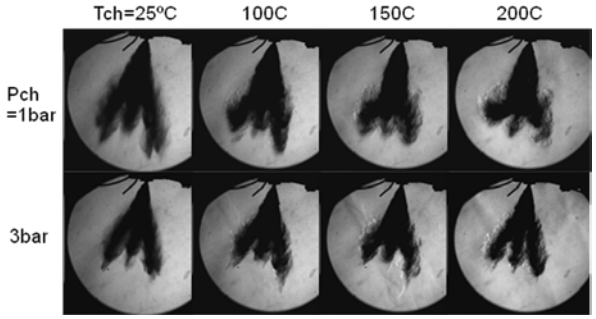

Figure 6. Effect of chamber temperature and pressure at 1.5ms ASOI.

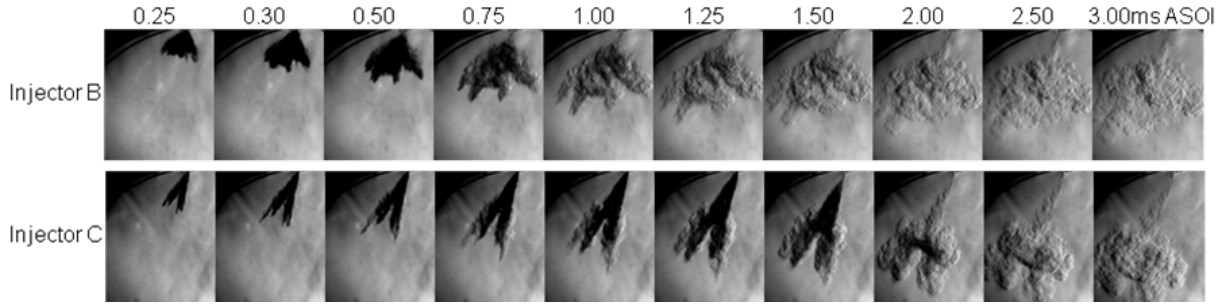

Figure 7. Schlieren spray images for Injector B and C.

Injector B and C were examined by Schlieren to evaluate the difference in the hole geometry (Fig. 7). The ambient temperature and pressure was 200ºC and 3bar respectively, and the mass of injected ethanol was fixed at 5mg for the testing. The fuel temperature was 60ºC. It was obvious that the plumes of smaller L/D (Injector B) developed slower and wider. Although slower evaporation of the spray of Injector B was expected because of larger SMD which is the result of larger hole diameter, complete evaporation of the spray of Injector B seems faster than Injector C. The reason can be considered that Injector B had larger spray targeting angle and it enlarged the available surface of the sprays for faster evaporation. Because of faster evaporation and larger diameter of the holes, Injector B was able to keep the mixture cloud near the nozzle exit, which is important to avoid excess wall wetting during engine operation.

The effect of fuel composition on the spray structure was examined with Injector A with the fixed injection duration of 1.5ms, and the result is shown in Fig. 8. The ambient condition was set to simulate a wormed up homogeneous condition with high Exhaust Gas Recirculation (EGR). The ambient temperature and pressure was 200ºC and 1bar, fuel temperature was 60ºC. At the early stage of injection (~1.0ms ASOI), separation of plumes in E50 and E100 spray was observed while the plumes of gasoline collapsed. E100 vapor was detected mainly at the bottom of the images at 3ms ASOI, although the vapor of gasoline was found to be widely distributed in the middle of the image. This result indicates that slow initiation of evaporation process of E100. The liquid fuel kept penetrating and traveled farther while the evaporated gas fuel lost its momentum and slowed down. The slow vaporization of ethanol can be considered as a result of relatively higher initial boiling point (IBP), which is 78.4ºC at 1bar. On the other hand, gasoline generally contains lighter hydrocarbons which boiling points are lower than ethanol.

The effect of fuel composition was studied quantitatively either. Penetration, projection area, and spray angle were measured from the results and documented. Only penetration result is shown in Fig. 9 as an example. The time started with the injection command signal, and actual injections begun after 0.3ms roughly. The figure shows the results from three identical tests for each fuel, and the results demonstrated very good consistency. Stable spray is the advantage of a multihole injector, and it was confirmed experimentally. By 0.3ms ASOI, spray penetrations were identical for all fuels. After that, the gasoline spray started evaporating and lost its momentum to slow down. Although the penetration of gasoline was shorter at the middle of the figure, it decelerated slower than the ethanol sprays as time elapsed. This may result from the heavier components of gasoline which have more resistance against evaporation and penetrated more than the single component ethanol spray. The shape of E50 penetration resembled E100, but it was slightly slower because of evaporation of the gasoline portion. Earlier initiation of evaporation of gasoline fuel resulted in smaller projection area and narrower spray angle. The difference in the spray angle was negligible at the upstream of the spray.

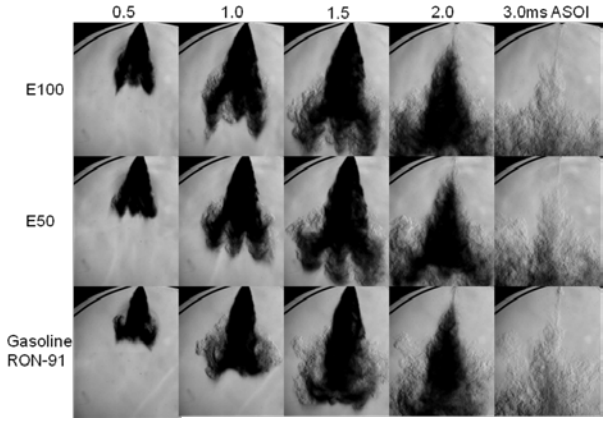

Figure 8. Effect of fuel composition for the fixed duration testing.

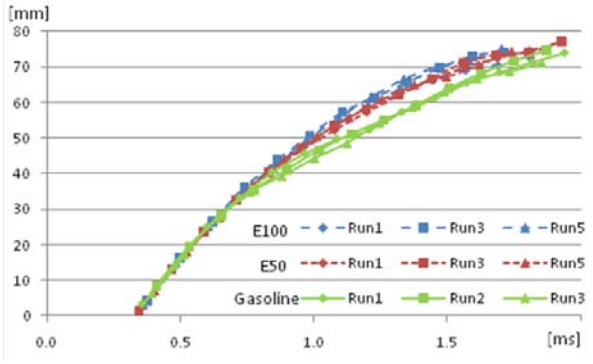

Figure 9. Penetration for the fixed duration testing.

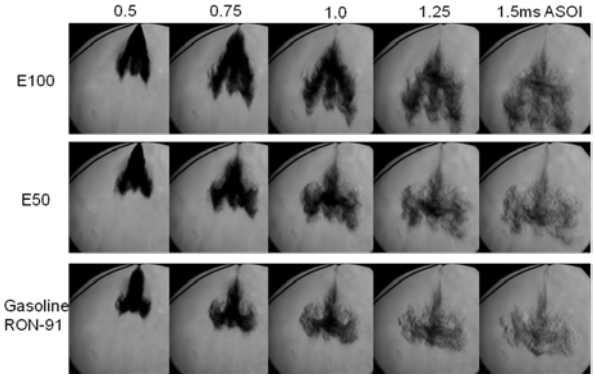

Figure 10. Effect of fuel composition for the fixed energy testing.

In addition, the fixed energy injection testing was carried out. The energy content of the injected fuel was kept constant to be equivalent to 5mg of gasoline. The injection mass and corresponding injection duration for each fuel were listed on Table 3. As a result of varying injection durations, the spray shapes of different fuels would be expected change significantly. The difference of fuels is clearly seen in Fig. 10 qualitatively. Both higher IBP and longer injection duration of ethanol injection enhance the spray penetration and projection area. Comparison of the results with gasoline spray at 1.5ms ASOI was summarized in Table 4. Increased penetration may lead to piston impingement and bore wetting resulting in increased hydrocarbon emissions and soot formation during engine operation. To minimize wall wetting, the injection timing must compensate for the effect of fuel composition.

Table 3. Fuel type and injected mass / pulse width (PW) for the equivalent energy injection.

Fuel Type	Mass / PW
Gasoline	5mg / 0.38ms
E50	6.2mg / 0.46ms
E100	8.0mg / 0.59ms

Table 4. Spray data comparison with gasoline spray at 1.5ms ASOI.

	Duration=1.5ms		Mass=5mg of gasoline or equivalent	
	E100	E50	E100	E50
Penetration	8%	6%	22%	8%
Projection Area	5%	6%	27%	12%
Spray Angle				
5mm	-1%	-1%	-	-
10mm	2%	0	-	-
20mm	7%	6%	-	-

The effect of fuel temperature on the spray structure was studied. The results for both ethanol and gasoline fuel are shown in the Appendix. The surrounding temperature and pressure were 210ºC and 1bar respectively. It is found that only little enhancement of vaporization was observed with the higher fuel temperature up to 60ºC. However, the plumes of ethanol collapsed at 80ºC and changed its appearance significantly. Again, this is due to flash boiling as the boiling point of ethanol at 1bar is 78.4ºC. In contrast, no flash boiling effect was observed for the spray of gasoline even if the fuel temperature increased.

Injector A and D were mounted on the OAE and the high-speed visualization was carried out for homogeneous charge operation. Since the regular projection lamps were used as the light sources, only liquid phase of the sprays was visible in the experiment due to Mie scattering. The injected fuel was 100% pure ethanol for all the OAE testing.

The in-cylinder CFD simulations of the OAE for both injectors were conducted, and the result for Injector D is displayed with the experimental results for comparison in Appendix. The simulation results show the distribution of the particles with radius information in color. The engine was motoring at 1000RPM, injection timing and quantity were 60CAD aTDC and 16mg respectively. The overall spray shape and the fuel distribution were comparable.

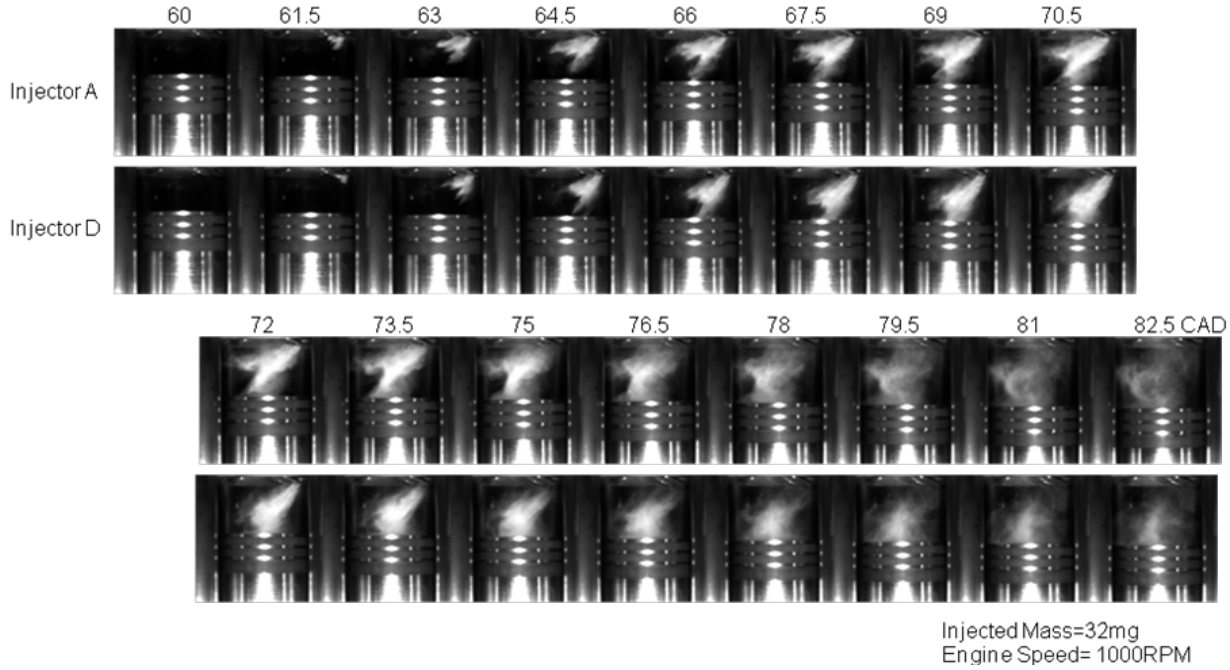

Figure 11. Homogeneous injection at 60CAD aTDC with different injector

An image sequence of every 1.5CAD for homogeneous injection is shown in Fig. 11. 32mg of ethanol was injected at 60CAD aTDC. The process of spray development and mixture formation inside the cylinder was well visualized. Comparison of two different injectors revealed that the mixture of Injector D had less tumble motion because Injector B was aiming the point closer to the center of the cylinder. Although stronger tumble motion is preferred for better mixing, sprays targeting far from the center will hit the cylinder walls and it can become the source of unburned hydrocarbon and soot emission. In fact, the revised spray targeting of Injector D was able to avoid the side wall wetting.

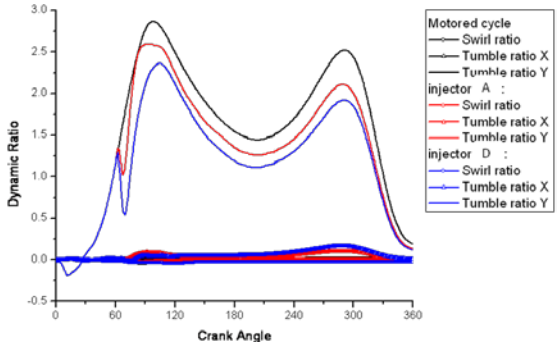

Figure 12. Dynamic ratio of homogeneous injection at 60CAD.

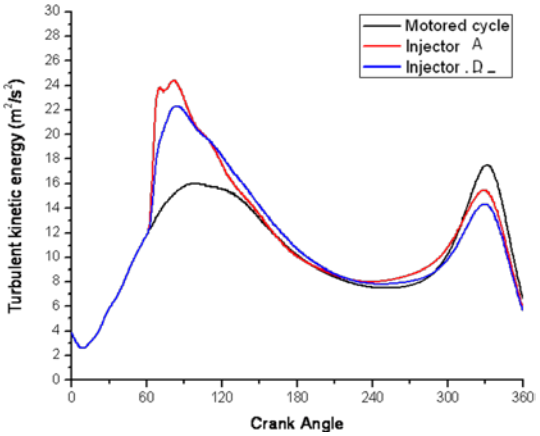

Figure 13. Turbulent kinetic energy of homogeneous injection at 60CAD.

The simulation results for the dynamic ratio and the turbulent kinetic energy calculated by CONVERGE were plotted in Figs. 12 and 13. It is reasonable that the in-cylinder flow has only one direction (Y) of tumble due to the engine design. Even though the trend of stronger tumble by Injector A was predicted by the experiment, it is found that the both injection killed the tumble motion and diminished it less than the motoring one because the direction of momentum of the spray was opposite to the direction of tumble. Less turbulent energy at the later part of the compression stroke was also observed for the injection at 60CAD.

Two other injection timings, 120 and 180CAD aTDC were tested to evaluate the effect of injection timing on mixing for the homogeneous operation. The test injector was Injector A. There was a significant difference between 60CAD and the other two conditions in terms of piston impingement. If the fuel was injected after 120CAD, no impingement was observed, which greatly helps improving combustion and reducing emission. Comparing 120 and 180CAD cases, a difference occurred in mixing after the injection finished. Fig. 14 shows images at 22.5CAD ASOI for each case along with the simulation result of the velocity vector plot at the center plane for the 120CAD injection. Since 120CAD is on the middle of intake stroke, dynamic in-cylinder flow caused by air induction can assist better mixing.

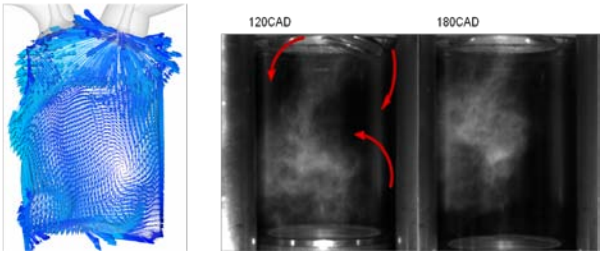

Figure 14. Effect of injection timing on mixing at 22.5CAD ASOI

The dynamic ratio and the turbulent kinetic energy for various injection timing are shown in Figs 15 and 16. For the injections of 120 and 180CAD, no more decrease of the tumble by the injection was observed. The tumble ratio was increased slightly at the time of injection, and was kept more than the motored cycle until the end of the compression stroke. Enhanced turbulent energy at the end of compression stroke, where the ignition takes place, is preferred for faster and cleaner combustion.

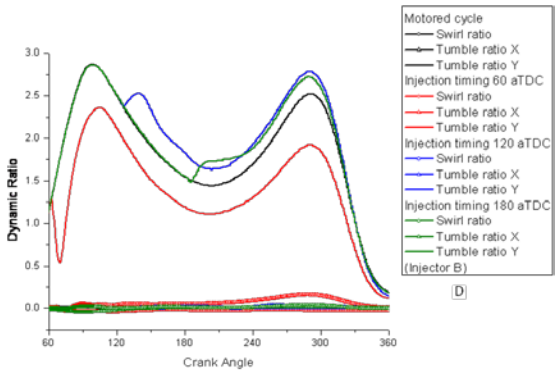

Figure 15. Dynamic ratio of homogeneous injection with Injector D at various timing.

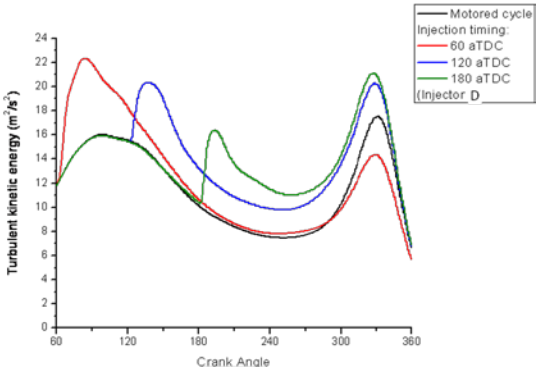

Figure 16. Turbulent kinetic energy of homogeneous injection with Injector D at various timing.

Conclusion

GDi injectors were tested with various ethanol content fuels in various conditions to evaluate the effects on the spray structure. Spray simulation by CONVERGE was also carried out. Following points were drawn as conclusions.

- Schlieren provided an effective technique for vapor phase visualization.
- The results of simulation by CONVERGE agreed fairly with the experimental data in terms of overall spray shape and penetration.
- At the ambient condition of high temperature and low pressure, flash boiling was observed. Flash boiling occurs when the fuel pressure instantly drops below the saturation pressure. This resulted in plume collapse and affected the spray targeting significantly.
- It was confirmed that the plumes of smaller L/D developed slower and wider. Spray of the injector with smaller L/D evaporated faster and the mixture cloud stayed closer to the nozzle exit for the fixed injection mass testing.
- Earlier initiation of evaporation for gasoline fuel and resultant spray collapse was observed.
- Slightly faster spray development was observed as the ethanol content in the fuel increased for the fixed duration comparison. The difference became clearer if the energy level of the injected fuel was fixed.
- Occurrence of flash boiling of the ethanol spray showed strong dependence on the fuel temperature due to its constant boiling point.
- Too early injection counteracted the tumble motion. The injection at the middle of the intake stroke increased the dynamic ratio and the turbulent energy at the point of ignition.

References

1. Zhao, F., M.-C. Lai, and D.L. Harrington, *Automotive spark-ignited direct-injection gasoline engines.* Progress in Energy and Combustion Science, 1999. **25**: p. 437-562.
2. Marriott, C.D., et al., *Development of a Naturally Aspirated Spark Ignition Direct-Injection Flex-Fuel Engine.* SAE Technical Paper 2008-01-0319, 2008.
3. Christie, M.J., N. Fortino, and H. Yilmaz, *Parameter Optimization of a Turbo Charged Direct Injection Flex Fuel SI Engine.* SAE Technical Paper 2009-01-0238, 2009.
4. Stein, R.A., C.J. House, and T.G. Leone, *Optimal Use of E85 in a Turbocharged Direct Injection Engine.* SAE Technical Paper 2009-01-1490, 2009.
5. Zhao, F.-Q., et al., *Spray Dynamics of High Pressure Fuel Injectors for DI Gasoline Engines.* SAE Technical Paper 961925, 1996.
6. Yamamoto, S., D. Tanaka, and K. Sato, *Keys to Understanding Spray-guided Combustion of a Narrow-spacing Gasoline Direct Injection SI Engine with a Centrally Mounted Multi-hole Injector.* SAE Technical Paper 2009-01-1497, 2009.
7. Dahlander, P. and R. Lindgren, *Multi-hole Injectors for DISI Engines: Nozzle Hole Configuration Influence on Spray Formation.* SAE Technical Paper 2008-01-0136, 2008.
8. Mitroglou, N., et al., *Spray Structure Generated by Multi-Hole Injectors for Gasoline Direct-Injection Engines.* SAE Technical Paper 2007-01-1417, 2007.
9. Das, S., S.-I. Chang, and J. Kirwan, *Spray Pattern Recognition for Multi-Hole Gasoline Direct Injectors Using CFD Modeling.* SAE Technical Paper 2009-01-1488, 2009.
10. Sato, K., et al., *Spray and Evaporation Characteristics of Multi-Hole Injector for DISI Engines -Effect of Diverging Angle Between Neighboring Holes.* SAE Technical Paper 2009-01-1500, 2009.
11. Kilic, A., L. Schulze, and H. Tschöke, *Influence of Nozzle Parameters on Single Jet Flow Quantities of Multi-Hole Diesel Injection Nozzles.* SAE Technical Paper 2006-01-1983, 2006.
12. Gold, M., et al., *Application of Optical Techniques to the Study of Mixture Preparation in Direct Injection Gasoline Engines and Validation of a CFD Model.* SAE Technical Paper 2000-01-0538, 2000.
13. Pickett, L.M., S. Kook, and T.C. Williams, *Visualization of Diesel Spray Penetration, Cool-Flame, Ignition, High-Temperature Combustion, and Soot Formation Using High-Speed Imaging.* SAE Technical Paper 2009-01-0658, 2009.
14. Arnaud, E., et al., *A Fluid Motion Estimator for Schlieren Image Velocimetry.* ECCV 2006, Lecture Notes in Computer Science, 2006. **3951**: p. 198-210.
15. Hori, T., et al., *Large Eddy Simulation of Non-Evaporative and Evaporative Diesel Spray in Constant Volume Vessel by Use of KIVALES.* SAE Technical Paper 2006-01-3334, 2006.
16. Yi, Y. and C.M. DeMinco, *Numerical Investigation of Mixture Preparation in a GDI Engine.* SAE Technical Paper 2006-01-3375, 2006.
17. Weber, J., et al., *Diesel Spray Characterization Using a Micro-Genetic Algorithm and Optical Measurements.* SAE Technical Paper 2006-01-1115, 2006.
18. Joh, M., et al., *Numerical Prediction and Validation of Fuel Spray Behavior in a Gasoline Direct-Injection Engine.* SAE Technical Paper 2001-01-3668, 2001.
19. Ricart, L.M., R.D. Reitz, and J. Deck, *Comparisons of Diesel Spray Liquid Penetration and Vapor Fuel Distribution With In-Cylinder Optical Measurements* Transactions of the ASME, 2000. **122**: p. 588-595.
20. Schmidt, D.P. and C.J. Rutland, *A New Droplet Collision Algorithm.* Journal of Computational Physics, 2000. **164**.
21. Han, Z. and R.D. Reitz, *Turbulence Modeling of Internal Combustion Engines Using RNG k −e Models.* Combust. Sci. and Tech, 1995. **106**.
22. Park, J.S., et al., *Visualization and Measurement of a Narrow-Cone DI Gasoline Spray for the Impingement Analysis.* International Journal of Automotive Technology, 2004. **5**: p. 221-238.
23. Serras-Pereira, J., et al., *Spray Development in a Direct-Injection Spark-Ignition Engine.* SAE Technical Paper 2007-01-2712, 2007.
24. Narumiya, H.H.a.K., M. Tsue, and T. Kadota, *Analysis of Initial Breakup Mechanism of Diesel Spray Injected into High-Pressure Ambience.* SAE Technical Paper 2004-01-0528, 2004.

Acknowledgements

The technical support from Convergent Science is greatly appreciated.

This material is based upon work supported by the Department of Energy under Award Number DE-FC26-07NT43270.

Appendix

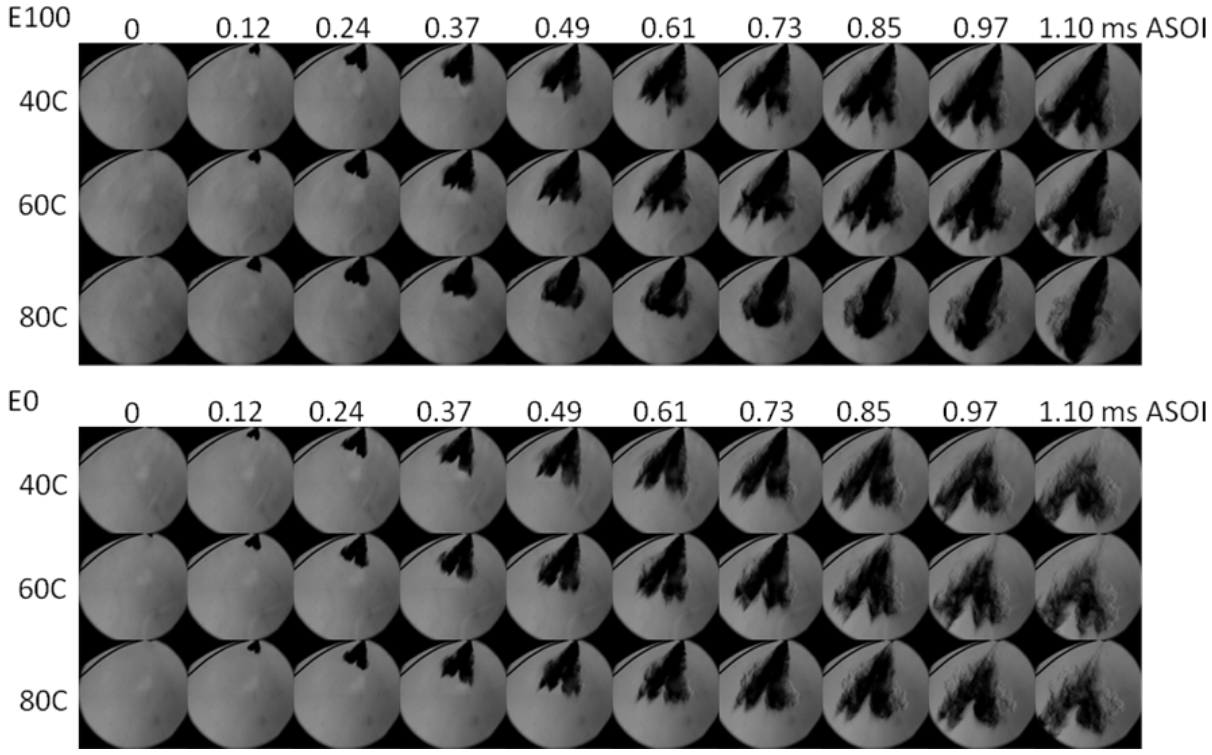

Figure A1. Effect of fuel temperature at 210ºC/1bar, 10mg of E0 or equivalent in energy.

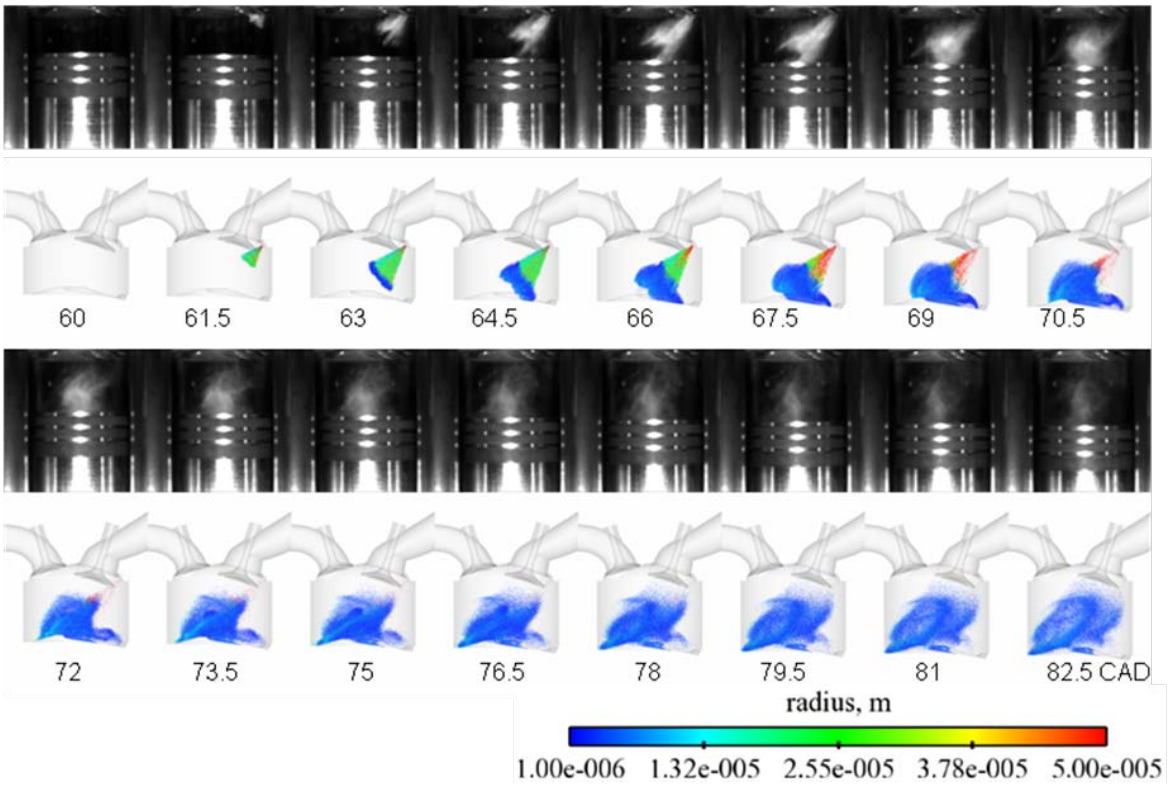

Figure A2. Comparison of CFD and experimental results of homogeneous injection at 60CAD aTDC with Injector D.